# Bortezomib inhibits proliferation, migration, and TGF-β1–induced epithelial–mesenchymal transition of RPE cells

Kun Moon,[1] Hyun-Gyo Lee,[2] Won-Ki Baek,[3,4] Youngkyun Lee,[5] Kwang Soo Kim,[2] Jong Hwa Jun,[2,3] Jae-Young Kim,[5] Choun-Ki Joo[6]

[1]Balgeunsesang Eye clinic, Seoul, South Korea; [2]Department of Ophthalmology, Keimyung University School of Medicine, Dongsan Medical Center, Daegu, South Korea; [3]Institute for Cancer Research, Keimyung University, Dongsan Medical Center, Daegu, South Korea; [4]Department of Microbiology, Keimyung University School of Medicine, Daegu, South Korea; [5]Department of Oral Biochemistry, School of Dentistry, IHBR, Kyungpook National University, Daegu, South Korea; [6]Department of Ophthalmology and Visual Science, Seoul St. Mary's Hospital, College of Medicine, The Catholic University of Korea, Seoul, South Korea

**Purpose:** Nuclear factor kappa B (NF-κB) plays an important role in the epithelial–mesenchymal transition (EMT) of RPE cells. We investigated the effects of a proteasome inhibitor, bortezomib, on the EMT in RPE cells. In addition, we assessed the influence of bortezomib on regulation of the NF-κB pathway during this process.
**Methods:** After treatment with various concentrations of bortezomib, cell viability was analyzed with the water-soluble tetrazolium salt-8 assay, cell-cycle regulation was evaluated with flow cytometry, and cell migration was monitored with in vitro wound healing and Transwell migration assays. To induce fibroblastoid transformation, the RPE cells were treated with recombinant human transforming growth factor (TGF)-β1 (10 ng/ml), and western blot and immunocyto-chemical analyses were performed to evaluate altered expression of EMT markers after treatment with bortezomib. To verify the effect of bortezomib on shrinkage by myofibroblastic transformation, a contraction assay of the RPE–collagen gel lattice was performed.
**Results:** Treatment with bortezomib decreased RPE viability in a dose-dependent manner, and flow cytometry revealed that these effects were due to arrest of the G2/M phase cell-cycle. In the in vitro wound healing and Transwell migration assays, treatment with 20 nM bortezomib significantly impeded RPE migration. Treatment with bortezomib also significantly inhibited TGF-β1-induced transdifferentiation of the RPE cells. The effects on proliferation, migration, and the EMT were mediated by regulation of the NF-κB signaling pathway. In addition, bortezomib inhibited contraction of the RPE–collagen gel lattices.
**Conclusions:** Bortezomib inhibits myofibroblastic transformation of RPE cells by downregulating NF-κB expression and prevents contraction of the RPE–collagen gel matrix. Thus, bortezomib represents a candidate putative therapeutic agent for management of retinal fibrotic diseases.

Human RPE cells are essential for visual functions that support photoreceptor function and regulate the blood–retina barrier (BRB) by forming mature tight junctions composed of zonular occludens-1 (ZO-1), occludin, and claudin family proteins [1,2]. After the completion of development in the early gestational period, RPE cells become dormant, undergoing minimal proliferation throughout life [2]. Dissociation of epithelial cells from their original locations promotes alterations in phenotypes and physiology, often accompanied by development of cellular plasticity, acquisition of migratory properties, loss of cell type-specific gene expression, and cytoskeletal rearrangements [3-5].

In ocular pathophysiology, such cellular processes are implicated in various fibrotic diseases. In proliferative

Correspondence to: Jong Hwa Jun, Department of Ophthalmology, Keimyung University School of Medicine, Dongsan Medical Center, Daegu, South Korea, Phone: 82-53-250-7708; FAX: 82-53-250-7705; email: junjonghwa@gmail.com

vitreoretinopathy (PVR), dispersion of RPE cells through the retinal breaks in rhegmatogenous retinal detachment (RRD) provides the opportunity to disseminate RPE cells into the subretinal space or vitreous cavity and induce inflammatory processes caused by breakdown of the BRB [6,7]. In addition, the epiretinal/subretinal membrane (ERM), or tractional membrane formations in proliferative diabetic retinopathy (PDR) accompanying RRD, habitual retinal cells, RPE cells, and glial cells are major sources of the ERM [8,9]. Moreover, RPE cells may play pathological roles in idiopathic ERM, although this remains controversial [10].

In these diseases, contraction of the fibrotic membrane is crucial for ERM or PVR pathology, and myofibroblastic transformation by epithelial–mesenchymal transition (EMT) of RPE cells is a hallmark of the associated pathobiology [11,12]. RPE cells are stimulated by various cytokines, including transforming growth factor (TGF)-β, platelet-derived growth factor (PDGF), vascular endothelial growth

factor, tumor necrosis factor α, and epidermal growth factor [6,7,13-15]. RPE cells that undergo dedifferentiation are transformed into myofibroblasts with accelerated proliferation and migration.

Nuclear factor kappa B (NF-κB) is a key transcriptional regulator of various responses and plays a pivotal role in regulation of inflammatory signaling cascades. NF-κB is activated by stress or injury, inflammatory cytokines, virus, and bacterial toxins, and downstream effectors of the NF-κB are involved in cellular proliferation, differentiation, and apoptosis [16]. Several drugs are used to regulate NF-κB in inflammatory diseases and tumors. Furthermore, fibrogenesis in multiple tissues can be inhibited by blockade of NF-κB [17,18]. Ocular fibrotic diseases, such as posterior capsule opacification, are associated with similar EMT pathobiology. Therefore, inhibition of NF-κB signaling by RNA silencing, sulfasalazine, or antisense oligodeoxynucleotide prevents these diseases [19-21]. NF-κB plays essential roles in induction and maintenance of EMT, and loss of NF-κB activity decreases EMT-related gene expression [22-24]. Together, these observations suggest that inhibition of NF-κB represents a promising therapeutic strategy for the prevention or control of ocular fibrotic diseases arising from EMT pathobiology.

Bortezomib (Velcade®; Millennium Pharmaceuticals Inc., Cambridge, MA) is a cancer drug approved by the U.S. Food and Drug Administration (FDA) for the treatment of multiple myeloma and mantle cell lymphoma as a proteasome inhibitor [25,26]. Bortezomib was originally developed as a blocker of proteasomal degradation of nuclear factor of kappa light polypeptide gene enhancer in B-cells inhibitor, alpha (IκBα), which acts by binding to the catalytic site of the 26S proteasome with high affinity and specificity; however, the precise mechanisms have not been fully elucidated [25-27].

In this study, we focused on the therapeutic effects of bortezomib on the EMT of RPE cells induced by TGF-β1, a potent inhibitor of the NF-κB signaling pathway [28]. We evaluated the inhibitory effects of bortezomib in an in vitro EMT model system consisting of RPE cells.

## METHODS

*Cell line and cell-culture treatments:* The immortalized human RPE line ARPE-19 was purchased from American Type Culture Collection (ATCC, Manassas, VA). Passage 19 cells were received and were used in experiments after five to ten more passages. ARPE-19 was maintained in 1:1 Dulbecco's modified eagle's medium/Ham's F12 nutrient (DMEM/F12; Welgene, Daegu, South Korea) supplemented with 10% (v/v) fetal bovine serum (FBS; Welgene) and 1%

(v/v) penicillin/streptomycin (Welgene) in a humidified incubator at 37 °C in 5% $CO_2$. To induce EMT, RPE cells at 90% confluence were treated with human recombinant TGF-β1 (10 ng/ml) in serum-free medium. Bortezomib was dissolved in dimethyl sulfoxide (DMSO), and the final concentration of DMSO in samples did not exceed 0.0002% (v/v). RPE cells were cultured with 20 nM bortezomib or the corresponding volume of DMSO (control).

*STR analysis:* Seventeen short tandem repeat (STR) loci plus the gender-determining locus, amelogenin, were analyzed in Cosmo genetech (Seoul, Korea) using GeneMapper® software 5(Applied Biosystems, Foster City, CA). Appropriate positive and negative controls were run and confirmed for each sample submitted. The STR analyses are presented in Appendix 1.

*Antibodies and reagents:* Reagents and kits were obtained from the following suppliers: bortezomib, Selleckchem (Houston, TX); human recombinant TGF-β1, PeproTech (Rocky Hill, NJ); Vectashield Mounting Medium with 4',6-diamidino-2-phenylindole (DAPI), Vector Labs (Burlingame, CA); a Cell Counting Kit-8 (CCK-8), Dojindo Molecular Technologies (Rockville, MD); inserts for Transwell migration assays, Corning (Corning, NY); a Collagen Gel Contraction Assay Kit, Cell Biolabs (San Diego, CA); and a Propidium Iodide Flow Cytometry Kit, Abcam (Cambridge, UK). Primary antibodies were as follows: anti-RHOG, Sigma (St. Louis, MO); anti-RAC1, EMD Millipore (Billerica, MA); anti-α-smooth muscle actin (SMA) and glyceraldehyde-3-phosphate dehydrogenase (GAPDH), Abcam; anti-NF-κB, phospho-NF-κB, IκBα, vimentin, ZO-1, N-cadherin, and β-catenin, Cell Signaling Technology (Danvers, MA); and anti-occludin, Santa Cruz Biotechnology (Dallas, TX). All secondary antibodies for the immunoblot assays were acquired from Jackson Laboratory (Bar Harbor, ME), and fluorescence-conjugated secondary antibodies for immunocytochemistry and Alexa Fluor 488 phalloidin were obtained from Thermo Fisher Scientific (Waltham, MA). All other chemicals were obtained from Sigma.

*Cell viability assay:* To determine the effective concentrations of bortezomib for regulation of RPE physiology, we plated ARPE-19 cells in four sets of 12-well plates and tested the effects of various concentrations of bortezomib (control [vehicle], 0.2, 2.0, and 20 nM) on cell viability at various time points (12, 24, 36, and 48 h). Every 12 h, the culture medium was aspirated, and the cells were rinsed with PBS (1X; 9 g/l NaCl, 0.21 g/l $KH_2PO_4$, 0.726 g/l $Na_2HPO_4 \cdot 7H_2O$, pH 7.2). CCK-8 reagent (100 μl) mixed with serum-free medium (900 μl) was added to each well. After 4-h incubation, 100 μl of the reagent/medium mixture was transferred to a 96-well

plate. Colorimetric detection at a wavelength of 450 nm was performed on a microplate reader (SPECTROstar Nano, BMG LABTECH GmbH, Ortenberg, Germany).

*Flow cytometry:* RPE cells were cultured in the presence or absence of 20 nM bortezomib for 24 or 48 h, and flow cytometric analysis was performed at each time point. For this purpose, culture medium was aspirated and rinsed with PBS, and 0.25% trypsin-EDTA solution was added to the cell monolayer to harvest the RPE cells as a single-cell suspension. After the cell pellets were spun down, the supernatant was aspirated, and the pellets were resuspended in PBS. The RPE cells were then fixed with 70% cold ethanol on ice and rehydrated with PBS. The fixed cells were stained with the propidium iodide and RNase mixture. Measurements were performed on a benchtop flow cytometer (NovoCyte Flow Cytometer Systems, ACEA Biosciences, San Diego, CA), and the results were analyzed using the NovoExpress software (ACEA Biosciences).

*Western immunoblot analyses:* After the culture medium was removed followed by three rinses with cold PBS, the cells were lysed using radioimmunoprecipitation assay (RIPA) buffer (ELPIS-Biotech Inc., Daejeon, South Korea). Equal quantities of each protein sample were loaded in lanes of 8–15% sodium dodecyl sulfate polyacrylamide gel electrophoresis (SDS–PAGE) gels, and the proteins were separated with electrophoresis. Resolved proteins were transferred to nitrocellulose membranes and blocked with 5% nonfat milk in a mixture of Tris-buffered saline (TBS) and Tween 20 (TBST) for 1 h. After overnight incubation with the indicated primary antibodies, the membranes were incubated with secondary antibodies for 1 h. Specific proteins were detected with enhanced chemiluminescence on a ChemiDoc™ MP System using Image Lab™ Software (Bio-Rad, Hercules, CA). GAPDH was used as a loading control for blot band densitometry. ImageJ software (freely available from the National Institutes of Health, Bethesda, MD) was used for densitometric analyses.

*Phalloidin staining and immunocytochemistry:* ARPE-19 cells were seeded in four-well glass cell-culture slides (SPL Life Sciences, Pocheon, Korea). The RPE cells were cultured in the presence or absence of 20 nM bortezomib at 24 h after plating and cultured to 50–60% confluence. After the medium was removed followed by three rinses with PBS, the cells were fixed with 4% paraformaldehyde for 30 min. For observations of filamentous actin, the cells were stained with Alexa Fluor 488–conjugated phalloidin/Vectashield mounting solution containing DAPI. For the immunocytochemical analyses, the cells were permeabilized with 0.4% (v/v) Triton X-100 for 15 min, and then blocked with 1% (w/v)

bovine serum albumin (BSA) in 0.1% (v/v) Tween-20/PBS for 30 min. Samples were incubated with primary antibodies for 12 h at 4 °C, followed by Alexa Fluor 488– or 594–conjugated secondary antibodies (Thermo Fisher Scientific) for 2 h at room temperature. The nuclei were stained with DAPI after several rinses. Each slide was observed on an inverted fluorescent microscope (Ti-U, Nikon Instruments Inc., Melville, NY), and images were taken using the NIS-Elements software (Nikon Instruments Inc.).

*In vitro wound-healing assay:* ARPE-19 cells were placed on 12-well plates and cultured to 90% confluence. Crosshair linear wounds were made with a standard 200-µl pipette tip. After three rinses with PBS, medium containing 1% FBS was added, and the cells were cultured in the presence or absence of 20 nM bortezomib. The remaining wound area was observed under a phase-contrast microscope every 12 h. The wound area at each time point was measured using ImageJ.

*Transwell migration assay:* ARPE-19 cells were trypsinized and resuspended in serum-free medium in the presence or absence of 20 nM bortezomib. Medium containing 10% FBS was added to each well (the bottom well), and the cell suspension was poured into polycarbonate membrane inserts with 8-µm pores (the top well). After 24-h incubation, cells that had migrated to the bottom side of the polycarbonate membrane were fixed with 4% paraformaldehyde and stained with hematoxylin. Migratory cells were counted under a phase-contrast microscope at three different locations on each insert.

*RPE–collagen gel contraction assay:* ARPE-19 cells were cultured in 100-mm dishes and harvested using 0.25% trypsin-EDTA solution. Two parts of cell suspension were mixed with eight parts of cold collagen gel solution, and then 100-µl aliquots of the cell/collagen gel mixture was dispensed into 48-well culture plates. After polymerization of the cell/gel mixture for 1 h at 37 °C, 100 µl of medium containing 20 ng/ml TGF-β1, with or without 20 nM bortezomib, was added to the top of the collagen lattice, and the samples were incubated for up to 72 h. Each gel was observed under a phase-contrast microscope, and the collagen gel area in each well was measured using images taken after 24 h of incubation. To evaluate cell spreading and cell-to-cell adhesion, each cell/collagen gel mixture was observed on an inverted microscope (Ti-U, Nikon Instruments Inc.). Images were acquired using the NIS-Elements imaging software (Nikon Instruments Inc.). The collagen gel area was measured using ImageJ.

*Statistical analysis:* Representative data were collected from at least triplicate experiments. All experiments were evaluated statistically with an independent *t* test or a one-way

ANOVA (ANOVA) test, and the Tukey HSD post-hoc test was applied to determine significant differences between results. A p value of less than 0.05 was regarded as statistically significant.

### RESULTS

*Bortezomib decreases RPE density:* Treatment of RPE cells with 20 nM bortezomib for 48 h resulted in significantly lower cell density relative to the control samples (Figure 1A). Therefore, to determine the effective working concentration of bortezomib, we treated the RPE cells with various concentrations of bortezomib (0, 0.2, 2.0, and 20 nM) and repeatedly measured cell viability every 12 h for 48 h. Bortezomib decreased cell viability in a dose-dependent manner; 20 nM bortezomib significantly decreased cell viability or density after 24 h, and this effect was maintained at 48 h (Figure 1B).

*Bortezomib induces arrest of the G2/M phase cell cycle:* After we treated the RPE cells with 20 nM bortezomib, we analyzed the cell cycle with flow cytometry. Treatment with bortezomib for 24 or 48 h increased the population of G2/M-arrested cells (Figure 1C,D). However, the proportion of sub-G1 cells was not significantly increased by treatment with bortezomib in comparison with vehicle-treated cells (data not shown). These results support that the decrease in cell viability, especially the abrupt change at the 20 nM concentration, was due to arrest in the G2/M phase.

*Bortezomib inhibits RPE migration:* To assess the effects of bortezomib on RPE migration, we performed in vitro wound-healing and Transwell migration assays. After 24 h in the presence of bortezomib, the remaining wound area was significantly larger than in the control wells. After treatment with bortezomib for 36 or 48 h, the wound area remained larger than in the control samples (Figure 2A,B). The results of the Transwell migration assay were in accordance with those of the wound-healing assay: The number of migrated cells was significantly lower in the bortezomib-treated samples (Figure 2C,D).

*Bortezomib regulates RPE motility by decreasing the number of lamellipodia via downregulation of RHOG/RAC1:* Based on the results of the migration and in vitro wound-healing assays, we hypothesized that treatment of RPE cells with bortezomib would affect factors related to cell motility. To test this idea, we performed phalloidin staining in the presence or absence of bortezomib. As we expected, bortezomib decreased the number of migratory organelles, including lamellipodia and stress fibers within the cytoplasm (Figure 2E). Western blot analysis showed that bortezomib downregulated expression of RHOG/RAC in RPE cells at early time points (Figure 2F). In addition, immunocytochemical staining revealed reduced expression of RHOG and RAC1 in RPE cells after treatment with bortezomib (Figure 2G).

*Bortezomib regulates various factors related to the EMT induced by TGF-β1:* Various concentrations of bortezomib were applied to RPE cells in which fibroblastoid
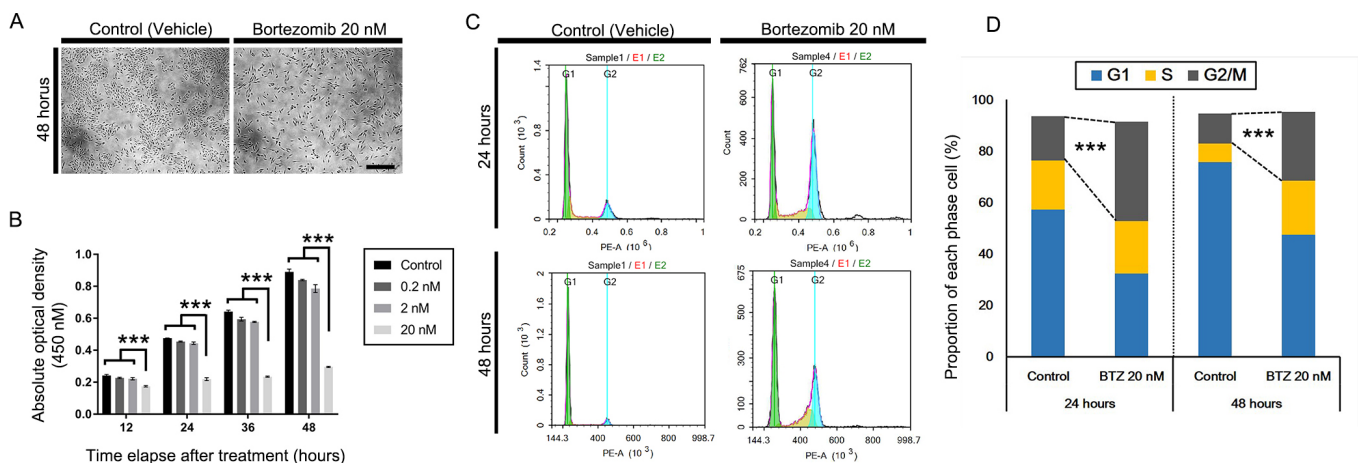


Figure 1. Effects of bortezomib on proliferation and cell cycle of APRE-19. **A**: Microscopic observations of a human RPE cell line (ARPE-19) in the presence or absence of 20 nM bortezomib. **B**: After various concentrations of bortezomib (0, 0.2, 2, and 20 nM) were applied, we evaluated cell viability with the water-soluble tetrazolium salt-8 (WST-8) assay. At a concentration of 20 nM bortezomib, cell viability was statistically significantly reduced (p<0.001). Data represent the mean ± standard deviation (SD) of three replicates. ***p<0.001 with one-way ANOVA, followed by Tukey's honest significant difference (HSD) post-hoc test. **C**: Flow-cytometric analysis revealed that bortezomib induced arrest of the G2/M phase at 24 and 48 h. **D**: After treatment with bortezomib, the proportion of RPE cells in the G2/M phase was statistically significantly higher than that in the control samples (p<0.001). ***p<0.001 with an independent *t* test, n=3, standard error.
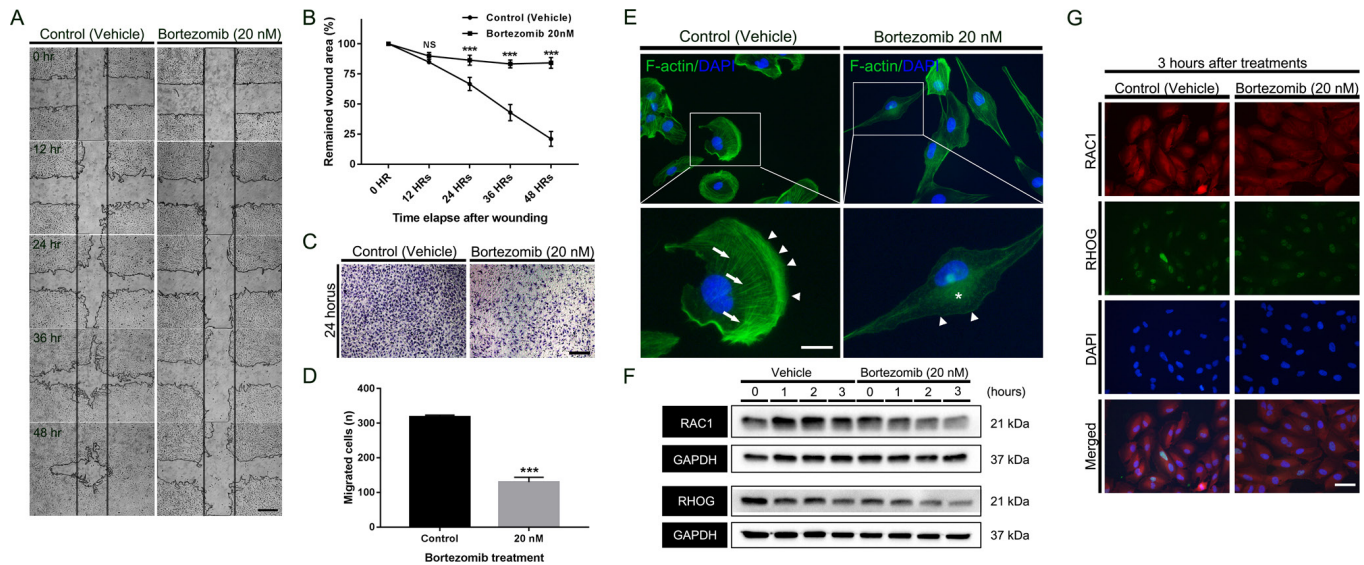
Figure 2. Effects of bortezomib on migration of APRE-19. **A**: In vitro wound-healing assay revealed that bortezomib, in comparison with vehicle, significantly inhibited wound healing in RPE monolayers. **B**: Quantification of the remaining wound area. Bortezomib inhibited wound healing after 24 h. ***p<0.001 with an independent *t* test. **C**: Transwell migration assays revealed that bortezomib decreased RPE migration. **D**: Quantification of migrated RPE cells revealed a statistically significant decrease in migration by treatment with 20 nM bortezomib compared to that of control cells. ***p<0.001 with an independent *t* test, n=3, standard error. **E**: Filamentous actin staining revealed that bortezomib decreased the number of stress fibers and lamellipodia involved in cell migration. **F**: Western blot analysis of RAC1 and RHOG revealed that bortezomib downregulated RAC1/RHOG expression. **G**: Immunocytochemical analysis confirmed that bortezomib downregulated RAC1/RHOG expression.

transdifferentiation had been induced by treatment with TGF-β1. At 20 nM bortezomib, epithelial markers such as ZO-1 and occludin were upregulated, whereas N-cadherin, vimentin, α-SMA, and β-catenin were downregulated (Figure 3A); band densitometry in the triplicate samples revealed these differences were statistically significant (Figure 3B). Similar patterns of expression were displayed in immunocytochemical analysis (Figure 3C). Thus, bortezomib effectively reversed the EMT in RPE cells.

*Bortezomib inhibits pathologic contraction in RPE–collagen gel lattices:* Matrix contraction plays a crucial role in the pathology of myofibroblastic transformation, especially in PVR or the ERM. Therefore, we investigated the effect of bortezomib on the contraction of the RPE–collagen gel lattices induced by TGF-β1. In the presence of 20 nM bortezomib, contraction of the collagen gel was significantly reduced, whereas the control-treated gels shrunk to approximately half of their initial area (Figure 4A). After 24 h, bortezomib effectively reduced shrinkage of the collagen gel lattices, and this effect remained statistically significant for 72 h (Figure 4B). Microscopic observations revealed that treatment with bortezomib reduced RPE spreading and cell-to-cell adhesion, which is the basis of the fibrous contraction band (Figure 4C). Filamentous actin staining with phalloidin

revealed that the formation of stress fibers, which contributes to contraction of the RPE–collagen gel lattice, was diminished by treatment with bortezomib (Figure 4D).

*Bortezomib downregulates NF-κB signaling cascades in the presence or absence of TGF-β1:* To determine whether treatment with the 20 nM bortezomib concentration could regulate the NF-κB signaling pathway in RPE cells stimulated or unstimulated with 10 ng/ml TGF-β1, we performed western blot analyses in the presence or absence of bortezomib. As shown in Figure 5A,B, 20 nM bortezomib inhibited expression of NF-κB (p65) and decreased the level of NF-κB phosphorylation. Conversely, bortezomib downregulated IκBα at early time points (Figure 5A,B). These regulatory patterns were observed regardless of whether the RPE cells were stimulated or unstimulated with TGF-β1. Accordingly, immunocytochemical staining 1 h after treatment with vehicle or bortezomib revealed decreased cytoplasmic expression of NF-κB but increased expression of IκBα in RPE cells, with or without application of TGF-β1 (Figure 5C,D).

## DISCUSSION

Bortezomib, a modified dipeptidyl boronic acid analog, is the first proteasome inhibitor drug approved for relapsed refractory multiple myeloma. Since bortezomib was approved in
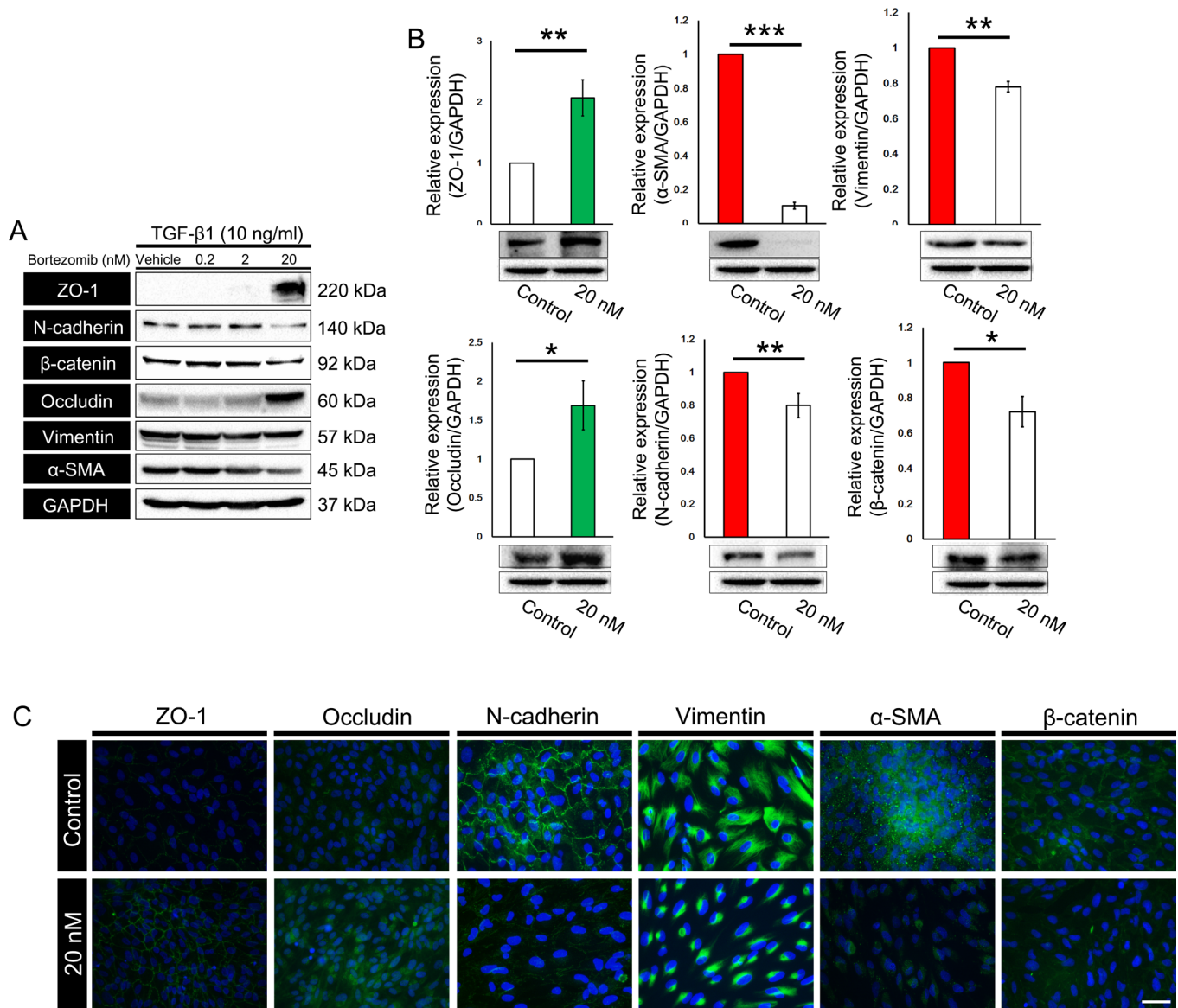
Figure 3. Regulations of bortezomib on epithelial-mesenchymal transition of APRE-19. **A**: Western blot analysis after treatment with various concentrations of bortezomib in the presence of transforming growth factor-β1 (TGF-β1, 10 ng/ml). At a concentration of 20 nM, treatment with bortezomib resulted in significant downregulation of mesenchymal factors (N-cadherin, α-smooth muscle actin [SMA], β-catenin, and vimentin) and upregulation of epithelial markers (ZO-1 and occludin). **B**: Quantification of western blot signals with densitometry. Bortezomib induced statistically significant upregulation of ZO-1 and occludin and downregulation of N-cadherin, α-SMA, β-catenin, and vimentin in the presence of TGF-β1. *$p < 0.05$, **$p < 0.01$, and ***$p < 0.001$ with an independent *t* test, n=3, standard error, **C**: Immunocytochemical analysis confirmed the western blot analysis results. Bortezomib (20 nM) statistically significantly increased the expression of ZO-1 and occludin and decreased that of N-cadherin, α-SMA, β-catenin, and vimentin in the presence of TGF-β1.

2003, it has been used as a first-line drug for this indication, either alone or in combination with other drugs [29]. Current clinical usage of bortezomib has been extended to treatment of thrombotic thrombocytopenic purpura and lymphoproliferative neoplasms, and recent reports showed that bortezomib used in concert with other agents promotes long-term survival of solid organ transplants [30-33]. In addition, several studies reported benefits of treatment with bortezomib in ophthalmic pathologies, such as experimental uveitis, ischemia-reperfusion injury, postoperative fibrosis in glaucoma filtration surgery, and retinoblastoma [34-38]. In this study, we investigated the inhibitory role of bortezomib in TGF-β1-induced EMT in RPE cells, which mimics the

PVR of rhegmatogenous retinal detachment or tractional ERM in diabetic retinopathy.

Initially, we tried to measure the minimal inhibitory concentration of bortezomib in the regulation of RPE physiologies. Cell viability analysis with the water-soluble tetrazolium salt-8 (WST-8) assay and microscopic observations showed that the 20 nM concentration of bortezomib clearly decreased cell density. However, because bortezomib can act as a cell-cycle regulator or an inducer of apoptosis [37,39], we cannot be sure whether the effects of the drug are mediated by arrest of the cell cycle or apoptosis. Therefore, we monitored the effect of the drug on cell-cycle progression, using flow cytometry. The results revealed that 20 nM bortezomib did not induce significant arrest in the sub-G1 phase in RPE cells but instead induced only arrest of the G2/M phase (data not shown).

In addition, we sought to determine with an in vitro cell scratch assay whether bortezomib could inhibit wound-healing ability. Although we limited the serum content of the culture medium, the results of the in vitro wound-healing assays reflect the proliferation and migration of cells. Therefore, to focus on migration, we also performed the Transwell migration assay. We observed that bortezomib effectively inhibited wound healing in RPE monolayers and that pure migration of RPE cells was also limited. For a detailed evaluation of RPE migration, we investigated alterations of the cytoskeleton by visualizing filamentous actin. Interestingly, bortezomib distinctively altered cytoplasmic actin and diminished lamellipodium formation at the cell border, and consequently, the RPE cells were elongated with the loss of polarity. Because such cytoskeletal regulation is governed by the RHOG/RAC1 signaling pathway, we assessed the effect of treatment with bortezomib on these factors and found that
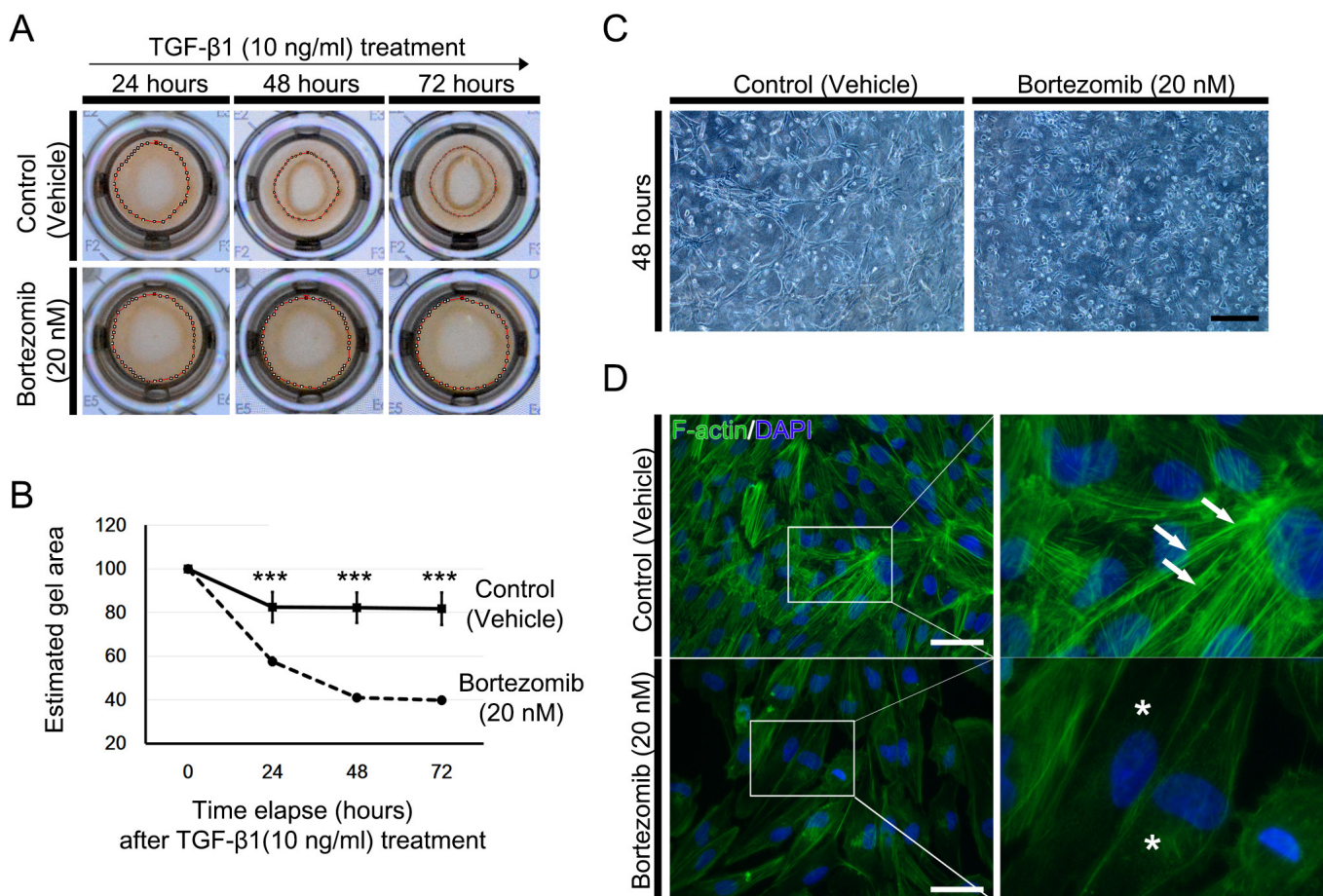


Figure 4. Inhibitory effect of bortezomib on RPE cell contraction. **A**: Contraction assay of the RPE–collagen gel complex in the presence or absence of 20 nM bortezomib. Bortezomib efficiently inhibited gel contraction. **B**: Statistical analysis of the gel area revealed that bortezomib decreased gel contraction after 24 h. \*\*\*p<0.001 with an independent *t* test, n=3, standard error. **C**: Microscopic observation revealed that cell spreading and cell-to-cell adhesion were impeded in the presence of bortezomib. **D**: Staining of filamentous actin revealed that the formation of stress fibers was inhibited in the presence of 20 nM bortezomib..

bortezomib downregulated the expression of RHOG and RAC1. It remains unclear whether the proteasome/NF-κB and RHOG/RAC1 pathways engage in crosstalk, and further evaluations are needed to confirm this relationship.

When activated, the NF-κB signaling pathway stimulates the production of various cytokines, including TGF-β [40,41]. TGF-β1 itself can also induce NF-κB signaling transduction by downregulating expression of IκBα [42]. Downregulation of NF-κB expression by proteasome inhibitors blocks transdifferentiation of human lens epithelial cells (LECs) [20,43]. Therefore, we predicted that bortezomib would also inhibit transdifferentiation of RPE cells via downregulation of NF-κB signaling transduction. Treatment with bortezomib downregulated NF-κB/phospho-NF-κB and upregulated IκBα expression in the presence or absence of TGF-β1. Furthermore, this agent also downregulated

mesenchymal factors, such as N-cadherin, vimentin, α-SMA, and β-catenin, but upregulated epithelial markers, such as ZO-1 and occludin. Together, these results showed that 20 nM bortezomib reversed the EMT process in a statistically significant manner.

Alterations in myofibroblasts promote pathologic contractile force during the EMT process. Therefore, blockade of matrix contraction is a crucial pharmacologic feature in the evaluation of drug effectiveness in the EMT process. We confirmed that bortezomib strikingly inhibited this pathologic process, preventing progression of matrix contraction even after 24 h. Microscopic observations supported this observation. RPE spreading and cell-to-cell adhesion were also significantly perturbed by treatment with bortezomib. Moreover, the migration assays indicated that NF-κB activity is suppressed by proteasome inhibition and
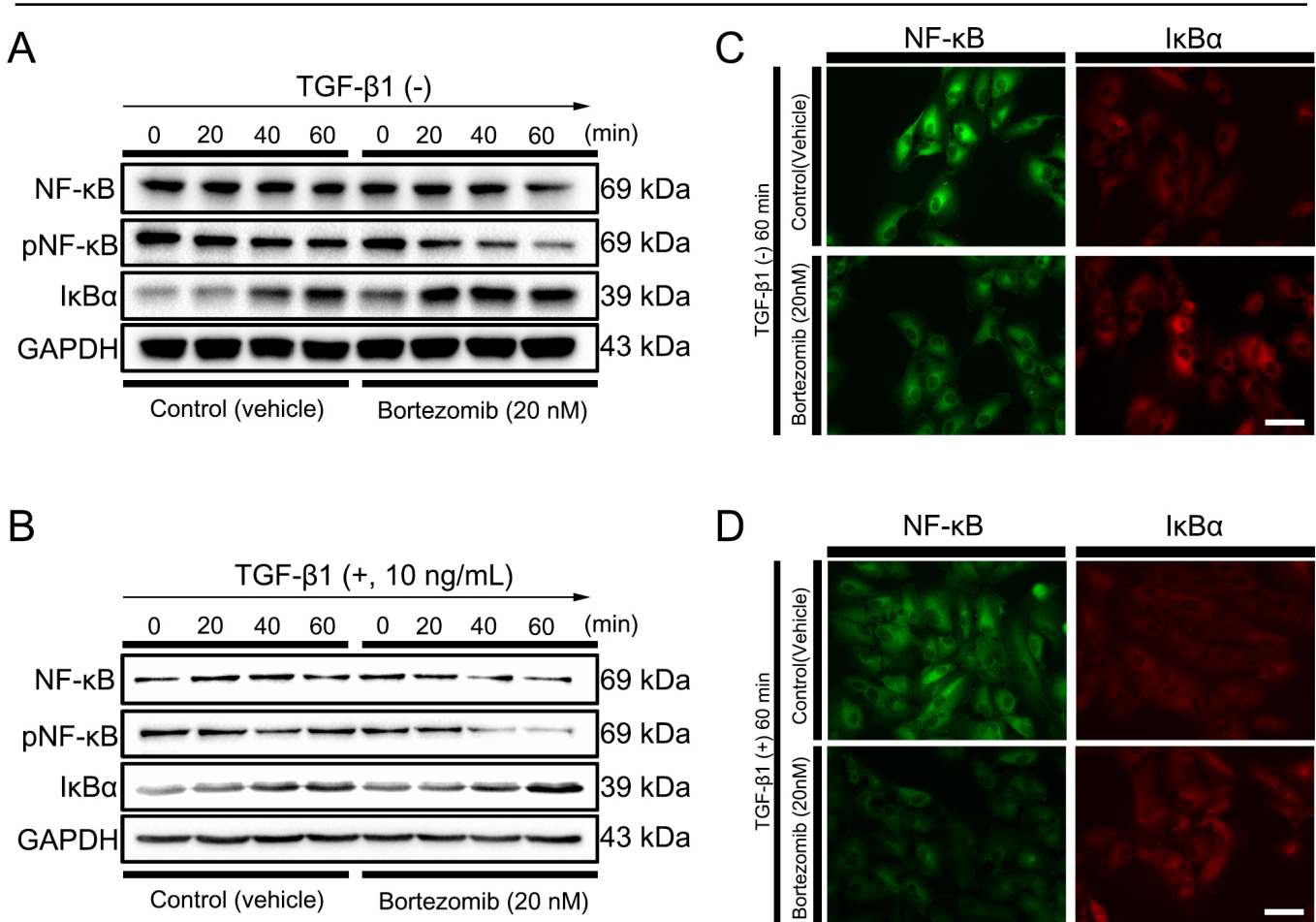


Figure 5. Regulation of NF-kB signaling pathway after treatment of bortezomib. Western blot analysis of the NF-κB signaling pathway in the absence **A** or presence **B** of TGF-β1. Bortezomib downregulated nuclear factor kappa B (NF-κB)/phospho-NF-κB expression and upregulated nuclear factor of kappa light polypeptide gene enhancer in B-cells inhibitor, alpha (IκBα) regardless of the presence of human transforming growth factor (TGF)-β1. **C**, **D**: Immunocytochemical staining at 60 min after the treatment with bortezomib yielded results similar to those for the western blot analysis.

that RHOG/RAC1 signal transduction plays an important role in this pathway.

In conclusion, bortezomib effectively inhibits proliferation, migration, and EMT induced by TGF-β1 in RPE cells. In particular, results showed that bortezomib has potential regulatory effects that inhibit tractional membrane formation and its pathologic contraction, which are the main pathologic processes underlying PVR or ERM. These results support the idea that bortezomib could be repositioned for treatment of intractable retinal diseases.

## APPENDIX 1. STR ANALYSIS.

To access the data, click or select the words "Appendix 1"

## ACKNOWLEDGMENTS

## REFERENCES

1.  Strauss O. The retinal pigment epithelium in visual function. Physiol Rev  2005; 85:845-81. [PMID: 15987797].

2.  Stern J, Temple S. Retinal pigment epithelial cell proliferation. Exp Biol Med (Maywood) 2015; 240:1079-86. [PMID: 26041390].

3.  Birchmeier C, Birchmeier W. Molecular aspects of mesenchymal-epithelial interactions. Annu Rev Cell Biol  1993; 9:511-40. [PMID: 8280470].

4.  Guarino M. Epithelial-to-mesenchymal change of differentiation. From embryogenetic mechanism to pathological patterns.  Histol Histopathol  1995; 10:171-84. [PMID: 7756736].

5.  Pagan R, Martin I, Alonso A, Llobera M, Vilaro S. Vimentin filaments follow the preexisting cytokeratin network during epithelial-mesenchymal transition of cultured neonatal rat hepatocytes. Exp Cell Res  1996; 222:333-44. [PMID: 8598222].

6.  Harada C, Mitamura Y, Harada T. The role of cytokines and trophic factors in epiretinal membranes: involvement of signal transduction in glial cells. Prog Retin Eye Res  2006; 25:149-64. [PMID: 16377232].

7.  Saika S, Yamanaka O, Flanders KC, Okada Y, Miyamoto T, Sumioka T, Shirai K, Kitano A, Miyazaki K, Tanaka S, Ikeda K. Epithelial-mesenchymal transition as a therapeutic target for prevention of ocular tissue fibrosis. Endocr Metab Immune Disord Drug Targets 2008; 8:69-76. [PMID: 18393925].

8.  Hiscott P, Gray R, Grierson I, Gregor Z. Cytokeratin-containing cells in proliferative diabetic retinopathy

9.  Pastor JC, de la Rua ER, Martin F. Proliferative vitreoretinopathy: risk factors and pathobiology.  Prog Retin Eye Res 2002; 21:127-44. [PMID: 11906814].

10.  Smiddy WE, Maguire AM, Green WR, Michels RG, de la Cruz Z, Enger C, Jaeger M, Rice TA. Idiopathic epiretinal membranes. Ultrastructural characteristics and clinicopathologic correlation. Ophthalmology 1989; 96:811-20. , discussion 821. [PMID: 2740079].

11.  Mitamura Y, Harada C, Harada T. Role of cytokines and trophic factors in the pathogenesis of diabetic retinopathy. Curr Diabetes Rev  2005; 1:73-81. [PMID: 18220584].

12.  Bu SC, Kuijer R, Li XR, Hooymans JM, Los LI. Idiopathic epiretinal membrane.  Retina  2014; 34:2317-35. [PMID: 25360790].

13.  Banerjee S, Savant V, Scott RA, Curnow SJ, Wallace GR, Murray PI. Multiplex bead analysis of vitreous humor of patients with vitreoretinal disorders.  Invest Ophthalmol Vis Sci  2007; 48:2203-7. [PMID: 17460280].

14.  Cui JZ, Chiu A, Maberley D, Ma P, Samad A, Matsubara JA. Stage specificity of novel growth factor expression during development of proliferative vitreoretinopathy.  Eye (Lond) 2007; 21:200-8. [PMID: 16531976].

15.  Lei H, Hovland P, Velez G, Haran A, Gilbertson D, Hirose T, Kazlauskas A. A potential role for PDGF-C in experimental and clinical proliferative vitreoretinopathy.  Invest Ophthalmol Vis Sci  2007; 48:2335-42. [PMID: 17460299].

16.  Chen F, Castranova V, Shi X, Demers LM. New insights into the role of nuclear factor-kappaB, a ubiquitous transcription factor in the initiation of diseases. Clin Chem 1999; 45:7-17. [PMID: 9895331].

17.  Oakley F, Meso M, Iredale JP, Green K, Marek CJ, Zhou X, May MJ, Millward-Sadler H, Wright MC, Mann DA. Inhibition of inhibitor of kappaB kinases stimulates hepatic stellate cell apoptosis and accelerated recovery from rat liver fibrosis. Gastroenterology  2005; 128:108-20. [PMID: 15633128].

18.  Oakley F, Teoh V, Ching ASG, Bataller R, Colmenero J, Jonsson JR, Eliopoulos AG, Watson MR, Manas D, Mann DA. Angiotensin II activates I kappaB kinase phosphorylation of RelA at Ser 536 to promote myofibroblast survival and liver fibrosis. Gastroenterology 2009; 136:2334-44. [PMID: 19303015].

19.  Lee SJ, Bae S, Seomun Y, Son MJ, Joo CK. The role of nuclear factor kappa B in lens epithelial cell proliferation using a capsular bag model.  Ophthalmic Res  2008; 40:273-8. [PMID: 18437038].

20.  Park HY, Kim IT, Lee KM, Choi JS, Park MO, Joo CK. Effects of nuclear factor-kappaB small interfering RNA on posterior capsule opacification.  Invest Ophthalmol Vis Sci  2010; 51:4707-15. [PMID: 20375325].

21.  Liu C, Wu XL, Wu XY, Zhang ZH, Liu XH. Effect of NF-kappaB p65 antisense oligodeoxynucleotide on transdifferentiation of normal human lens epithelial cells induced by

transforming growth factor-beta2. Int J Ophthalmol 2016; 9:29-32. [PMID: 26949606].

22. Huber MA, Azoitei N, Baumann B, Grunert S, Sommer A, Pehamberger H, Kraut N, Beug H, Wirth T. NF-kappaB is essential for epithelial-mesenchymal transition and metastasis in a model of breast cancer progression. J Clin Invest 2004; 114:569-81. [PMID: 15314694].

23. Kumar M, Allison DF, Baranova NN, Wamsley JJ, Katz AJ, Bekiranov S, Jones DR, Mayo MW. NF-kappaB regulates mesenchymal transition for the induction of non-small cell lung cancer initiating cells. PLoS One 2013; 8:e68597-[PMID: 23935876].

24. Cichon MA, Radisky DC. ROS-induced epithelial-mesenchymal transition in mammary epithelial cells is mediated by NF-kB-dependent activation of Snail. Oncotarget 2014; 5:2827-38. [PMID: 24811539].

25. Hideshima T, Richardson P, Chauhan D, Palombella VJ, Elliott PJ, Adams J, Anderson KC. The proteasome inhibitor PS-341 inhibits growth, induces apoptosis, and overcomes drug resistance in human multiple myeloma cells. Cancer Res 2001; 61:3071-6. [PMID: 11306489].

26. Tucker D, Rule S. Novel agents in mantle cell lymphoma. Expert Rev Anticancer Ther 2017; 17:491-506. [PMID: 28480764].

27. Bonvini P, Zorzi E, Basso G, Rosolen A. Bortezomib-mediated 26S proteasome inhibition causes cell-cycle arrest and induces apoptosis in CD-30+ anaplastic large cell lymphoma. Leukemia 2007; 4838-42. Epub 2007 Feb 1[PMID: 17268529].

28. Ocio EM, Mateos MV, Maiso P, Pandiella A, San-Miguel JF. New drugs in multiple myeloma: mechanisms of action and phase I/II clinical findings. Lancet Oncol 2008; 9:1157-65. [PMID: 19038762].

29. Kouroukis CT, Baldassarre FG, Haynes AE, Imrie K, Reece DE, Cheung MC. Cancer Care Ontario Hematology Disease Site Group. Bortezomib in multiple myeloma: a practice guideline. Clin Oncol (R Coll Radiol) 2014; 26:110-9. [PMID: 24321107].

30. Paterno F, Shiller M, Tillery G, O'Leary JG, Susskind B, Trotter J, Klintmalm GB. Bortezomib for acute antibody-mediated rejection in liver transplantation. Am J Transplant 2012; 12:2526-31. [PMID: 22681986].

31. Shah N, Meouchy J, Qazi Y. Bortezomib in kidney transplantation. Curr Opin Organ Transplant 2015; 20:652-6. [PMID: 26536428].

32. Cheah CY, Seymour JF, Wang ML. Mantle Cell Lymphoma. J Clin Oncol 2016; 34:1256-69. [PMID: 26755518].

33. Eskazan AE. Bortezomib therapy in patients with relapsed/refractory acquired thrombotic thrombocytopenic purpura. Ann Hematol 2016; 95:1751-6. [PMID: 27590601].

34. Poulaki V, Mitsiades CS, Kotoula V, Negri J, McMillin D, Miller JW, Mitsiades N. The proteasome inhibitor bortezomib induces apoptosis in human retinoblastoma cell lines in vitro. Invest Ophthalmol Vis Sci 2007; 48:4706-19. [PMID: 17898295].

35. Chung EJ, Moon SW, Jung SA, Cho YJ, Kim SW, Lee JH. Potentiation of bortezomib-induced apoptosis by TGF-beta in cultured human Tenon's fibroblasts: contribution of the PI3K/Akt signaling pathway. Invest Ophthalmol Vis Sci 2010; 51:6232-7. [PMID: 20702821].

36. Chen FT, Liu YC, Yang CM, Yang CH. Anti-inflammatory effect of the proteasome inhibitor bortezomib on endotoxin-induced uveitis in rats. Invest Ophthalmol Vis Sci 2012; 53:3682-94. [PMID: 22538426].

37. Chen FT, Yang CM, Yang CH. The protective effects of the proteasome inhibitor bortezomib (velcade) on ischemia-reperfusion injury in the rat retina. PLoS One 2013; 8:e64262-[PMID: 23691186].

38. Hsu SM, Yang CH, Shen FH, Chen SH, Lin CJ, Shieh CC. Proteasome inhibitor bortezomib suppresses nuclear factor-kappa B activation and ameliorates eye inflammation in experimental autoimmune uveitis. Mediators Inflamm 2015; 2015:847373-[PMID: 25653480].

39. Xia Y, Shen S, Verma IM. NF-kappaB, an active player in human cancers. Cancer Immunol Res 2014; 2:823-30. [PMID: 25187272].

40. Baeuerle PA, Henkel T. Function and activation of NF-kappa B in the immune system. Annu Rev Immunol 1994; 12:141-79. [PMID: 8011280].

41. Wang XC, Jobin C, Allen JB, Roberts WL, Jaffe GJ. Suppression of NF-kappaB-dependent proinflammatory gene expression in human RPE cells by a proteasome inhibitor. Invest Ophthalmol Vis Sci 1999; 40:477-86. [PMID: 9950608].

42. Arsura M, Wu M, Sonenshein GE. TGF beta 1 inhibits NF-kappa B/Rel activity inducing apoptosis of B cells: transcriptional activation of I kappa B alpha. Immunity 1996; 5:31-40. [PMID: 8758892].

43. Hosler MR, Wang-Su ST, Wagner BJ. Role of the proteasome in TGF-beta signaling in lens epithelial cells. Invest Ophthalmol Vis Sci 2006; 47:2045-52. [PMID: 16639014].